Retarded Casimir-Polder force on an atom near reflecting microstructures.

Article (Published Version)

Retarded Casimir-Polder force on an atom near reflecting microstructures

Claudia Eberlein and Robert Zietal
Department of Physics & Astronomy, University of Sussex, Falmer, Brighton BN1 9QH, United Kingdom
(Received 30 April 2009; published 15 July 2009)

We derive the fully retarded energy shift of a neutral atom in two different geometries that are useful for modeling etched microstructures. First, we calculate the energy shift due to a reflecting cylindrical wire, and then we work out the energy shift due to a semi-infinite reflecting half-plane. We analyze the results for the wire in various limits of the wire radius and the distance of the atom from the wire, and obtain simple asymptotic expressions useful for estimates. For the half-plane we find an exact representation of the Casimir-Polder interaction in terms of a single fast converging integral, which is easy to evaluate numerically.

DOI: 10.1103/PhysRevA.80.012504 PACS number(s): 31.70.−f, 41.20.Cv, 42.50.Pq

I. INTRODUCTION

The explosive rate of developments in nanotechnology as well as in the manipulation of cold atoms has meant that interest in atom-surface interactions has increased strongly in recent years. What were once tiny elusive effects are now dominant interactions, or, as the case may be, a major nuisance in some experimental setups. Motivated by a common type of microstructure, which consists of a protruding ledge fabricated by successive etching and possibly a thin electroplated top layer, we have recently studied the force on a neutral atom in close proximity of reflecting surfaces of either cylindrical geometry or that of a semi-infinite half-plane [1]. In the absence of free charges or thermal excitations, the interaction of the atom with the microstructure is dominated by Casimir-Polder forces [2], which are due to the interaction of the atomic dipole with polarization fluctuations excited by vacuum fluctuations of the electromagnetic field. If the atom is sufficiently close to the surface of the microstructure, then the interaction between the atomic dipole and the surface is purely electrostatic and retardation can be neglected, which was the case investigated in Ref. [1]. Then one does not need to quantize the electromagnetic field but can work with the classical Green's function of Poisson's equation. The only difficulty lies then in the geometry of the problem.

However, in experimental situations one more often finds that retardation is in fact important, as the distance of the atom from the surface of the microstructure is often commensurate or larger than the wavelength of a typical atomic transition. This is the case we investigate here, again for microstructures of two types of geometries: a cylindrical reflector of radius R and infinite length, and a reflecting half-plane.

Various versions of this problem have been studied before, both analytically and numerically. Probably the first to consider the interaction between an atom and a metallic wire, according to [3], was Zel'dovich [4] almost 75 years ago. This problem was then revisited and extended by Nabutovskii *et al.* [5], and subsequently by Marvin and Toigo [6]. In Nabutovskii's paper a dielectric cylinder is envisaged to be surrounded by a cylindrical shell of vacuum, which in turn is surrounded by a rarefied gas of polarizable particles. The interaction energy of a single particle is then calculated through the work done by the force (obtained from the stress tensor) due to the fluctuating electromagnetic fields, in the limit of zero density of the surrounding gas. The asymptotic results obtained there {Eqs. (23) and (24) of Ref. [5]} are, according to Ref. [3], valid only for dilute dielectric materials; they diverge in the perfect-reflector limit.

On the other hand, the work by Marvin and Toigo [6], motivated by [7,8] and based on a normal-mode expansion and a linear-response formalism [9], gives the same general formula for the interaction between a point particle and a cylinder [their Eq. (4.10)] as the equivalent result in [5]. We have no reason to believe that the result in [6] is incorrect in the perfect-conductor limit, as it reduces to our previous result [1] in the electrostatic limit. Moreover, Ref. [6] manages to recover the original Casimir-Polder result [2] in the large-radius limit of the cylinder. This suggests that the general expression in [5] is probably correct, only that the perfect-conductor limit does not commute with the asymptotic limit of the zero radius (or large distance of the atom from the cylinder) studied there. In the small-radius limit, the result for the interaction between an atom and a metallic filament, in both retarded and nonretarded limits, is also given by [3].

Marvin and Toigo's work [6] is certainly the most comprehensive but due to its generality it is also quite cumbersome to apply, which is mainly done numerically for just a few examples [10]. Further numerical studies of the interaction of atoms with macroscopic cylinders can be found in Refs. [11–14].

By contrast, in this paper we are after a relatively simple theory that allows one to estimate the force between an atom and a cylindrical reflector at any distance and cylinder radius. To this end we are not interested in the precise dependence of the interaction on material constants of the reflector, and therefore we work with the model of a perfectly reflecting surface.

As discussed in Ref. [1], we also determine the force between an atom and a semi-infinite half-plane in order to facilitate estimates for common types of microstructures that consist of a ledge protruding from a substrate. The Casimir-Polder interaction between an atom and such a half-plane has also been studied before but only in the extreme retarded limit of very large distances of the atom from the surface [15]. To the best of our knowledge no formula for the interaction in the intermediate region, when the distance of the atom from the surface is comparable to the typical wavelength of an internal transition in the atom, has been derived

yet. Recent work of Mendes *et al.* [16], dealing with wedges, does not include the general result in the half-plane geometry as a limiting case of a zero-angle wedge.

II. FIELD QUANTIZATION AND THE ENERGY SHIFT

The complete system of an atom interacting with the quantized electromagnetic field is described by the Hamiltonian

$$H = H_{\mathrm{Atom}} + H_{\mathrm{Field}} + H_{\mathrm{Int}}. \tag{1}$$

We choose to work with $\boldsymbol{\mu}\cdot\mathbf{E}$ coupling, i.e., our interaction Hamiltonian is

$$H_{\mathrm{Int}} = -\boldsymbol{\mu}\cdot\mathbf{E}. \tag{2}$$

Quantization of the electromagnetic field is done by way of a normal-mode expansion of the vector potential in terms of photon annihilation and creation operators for each mode λ and polarization σ,

$$\mathbf{A}(\mathbf{r},t) = \sum_{\lambda,\sigma} \frac{1}{\sqrt{2\varepsilon_0\omega_\lambda}}[a_\lambda^{(\sigma)}\mathbf{F}_\lambda^{(\sigma)}(\mathbf{r})e^{-i\omega t} + \mathrm{H.c.}]. \tag{3}$$

To describe a mode we use the composite index λ instead of a wave vector, as we shall be working in cylindrical coordinates where the quantum number of the azimuthal part of the mode function is discrete but the other two are continuous. We work in Coulomb gauge, $\boldsymbol{\nabla}\cdot\mathbf{A}(\mathbf{r})=0$, so that the normal modes $\mathbf{F}(\mathbf{r})$ satisfy the Helmholtz equation,

$$(\boldsymbol{\nabla}^2 + \omega^2)\mathbf{F}(\mathbf{r}) = \mathbf{0}. \tag{4}$$

The energy-level shift due to interaction (2) can be calculated perturbatively. For our system in state $|i;0\rangle$, i.e., the atom in state $|i\rangle$ and the electromagnetic field in its vacuum state $|0\rangle$, the lowest nonvanishing order of perturbation theory is the second, so that

$$\Delta W = \sum_{j\neq i} \frac{|\langle j;1_\lambda^{(\sigma)}| -\boldsymbol{\mu}\cdot\mathbf{E}|i;0\rangle|^2}{E_i - (E_j+\omega_\lambda)}. \tag{5}$$

As the relevant field modes can be expected to vary slowly over the size of the atom, we make the electric-dipole approximation, which simplifies the expression for the energy shift to

$$\Delta W = -\sum_{\lambda,\sigma,j\neq i} \frac{\omega_\lambda}{2\varepsilon_0} \frac{|\langle j|\boldsymbol{\mu}|i\rangle\cdot\mathbf{F}_\lambda^{(\sigma)*}(\mathbf{r})|^2}{E_{ji}+\omega_\lambda}, \tag{6}$$

where we have introduced the abbreviation $E_{ji}\equiv E_j - E_i$. The sum over intermediate states j in Eq. (6) is in practice limited to one or a few states to which there are strong dipole transitions from the initial state i. These strong dipole transitions dominate the internal dynamics of the atom, and the corresponding time scales are then given by $1/E_{ji}$, the inverse frequency of these dominant dipole transitions. Therefore, when we analyze the distance dependence of the energy shift, we shall use $1/E_{ji}$ for these transitions as the scale in which to compare the distance of the atom from the surface. We shall refer to E_{ji} as the frequency of a typical atomic transition.

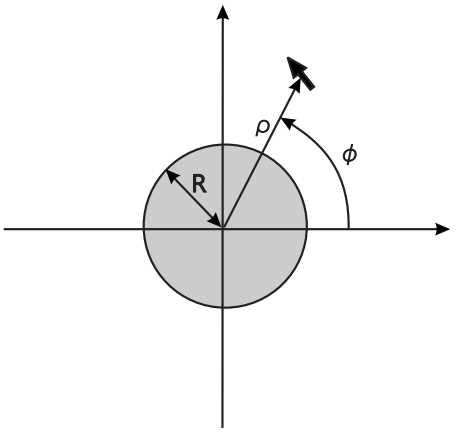

FIG. 1. Atomic electric-dipole moment in the vicinity of a perfectly reflecting cylinder of radius R. The normal modes $\mathbf{F}_\lambda^{(\sigma)}(\mathbf{x})$ in this geometry are given by Eqs. (15) and (16).

Alternatively one can use the atomic polarizability, whose diagonal elements are

$$\alpha_{\nu\nu}(\omega) = \sum_j \frac{2E_{ji}|\langle j|\mu_\nu|i\rangle|^2}{E_{ji}^2 - \omega^2}, \tag{7}$$

and express the energy shift as an integral over the polarizability and the electric field susceptibility at imaginary frequencies [17]. In this formalism one can see most easily that the energy shift at large distances (in the so-called retarded limit) must always depend just on the static polarizability

$$\alpha_{\nu\nu}(0) = \sum_j \frac{2|\langle j|\mu_\nu|i\rangle|^2}{E_{ji}}. \tag{8}$$

For brevity and presentational clarity we shall henceforth abbreviate the matrix elements of the atomic dipole moment as

$$|\boldsymbol{\mu}| \equiv |\langle j|\boldsymbol{\mu}|i\rangle|. \tag{9}$$

III. ENERGY SHIFT NEAR A PERFECTLY REFLECTING WIRE

First we wish to calculate the energy shift of an atom near a perfectly reflecting and infinitely long cylindrical wire of radius R. It is advantageous to work in cylindrical coordinates, cf. Fig. 1.

In order to find two independent transverse vector field solutions of Eq. (4), we make use of the representation theorem for the vector Helmholtz equation {Eq. 10.411 of [18]}. If $\Phi(\mathbf{x})$ is a solution of the scalar Helmholtz equation then the two independent solutions of the vector equation are given by

$$\mathbf{F}^{(1)}(\mathbf{r}) = (\boldsymbol{\nabla}\times\hat{\mathbf{e}}_z)\Phi(\mathbf{r}), \tag{10}$$

$$\mathbf{F}^{(2)}(\mathbf{r}) = \frac{1}{\omega}\boldsymbol{\nabla}\times(\boldsymbol{\nabla}\times\hat{\mathbf{e}}_z)\Phi(\mathbf{r}). \tag{11}$$

The particular choice of the constant unit vector $\hat{\mathbf{e}}_z$ is motivated by the symmetry of our problem, and lets us identify

the solutions $\mathbf{F}^{(1)}(\mathbf{r})$ and $\mathbf{F}^{(2)}(\mathbf{r})$ with the transverse electric (TE) and transverse magnetic (TM) modes, respectively. In cylindrical coordinates the scalar Helmholtz equation has solutions of the form

$$\Phi(\rho,\phi,z) = N[\cos\ \delta_m J_m(k\rho) + \sin\ \delta_m Y_m(k\rho)]e^{im\phi+i\kappa z}, \tag{12}$$

where $J_m(k\rho)$ and $Y_m(k\rho)$ are Bessel functions of the first and second kinds (Chapter 9 of [19]). The separation constants satisfy $\omega^2=k^2+\kappa^2$, and m is an integer. The phase shifts δ_m describe the superposition of regular and irregular solutions. In free space only regular solutions $J_m(k\rho)$ are admissible, and $\delta_m=0$. In the presence of the perfectly reflecting wire, the phase shifts serve to make the electromagnetic fields satisfy the boundary conditions on the surface of the wire. The normalization constant N is chosen such that

$$\int d^3\mathbf{r}\mathbf{F}^{(\sigma)*}_{\lambda'}(\mathbf{r})\cdot\mathbf{F}^{(\sigma)}_{\lambda}(\mathbf{r}) = \delta_{mm'}\delta(\kappa-\kappa')\frac{\delta(k-k')}{\sqrt{kk'}} \tag{13}$$

is met. Setting $\cos\ \delta_m=1$, $\sin\ \delta_m=0$, one can derive quite easily that $N=(2\pi k)^{-1}$.

On the surface of a perfect conductor, the tangential components of the electric field and the normal component of the magnetic field vanish. Therefore, at the surface $\rho=R$ of the cylindrical wire we must have $E_\phi=0=E_z$ and $B_\rho=0$. These boundary conditions determine the phase shifts as

$$\tan\ \delta_m^{\mathrm{TE}} = -\frac{J'_m(kR)}{Y'_m(kR)}, \quad \tan\ \delta_m^{\mathrm{TM}} = -\frac{J_m(kR)}{Y_m(kR)}. \tag{14}$$

According to Eqs. (10)–(12), the normalized mode functions $\mathbf{F}^{(\sigma)}_{\lambda}(\mathbf{r})$, $\lambda=\{k,m,\kappa\}$, that satisfy the boundary conditions at $\rho=R$, are given by

$$\mathbf{F}^{\mathrm{TE}}_{\lambda}(\rho,\phi,z) = \frac{1}{2\pi}\left[\frac{im}{k\rho}\frac{J_m(k\rho)Y'_m(kR)-Y_m(k\rho)J'_m(kR)}{\sqrt{J'^2_m(kR)+Y'^2_m(kR)}}\hat{\mathbf{e}}_\rho - \frac{J'_m(k\rho)Y'_m(kR)-Y'_m(k\rho)J'_m(kR)}{\sqrt{J'^2_m(kR)+Y'^2_m(kR)}}\hat{\mathbf{e}}_\phi\right]e^{im\phi+i\kappa z}, \tag{15}$$

$$\mathbf{F}^{\mathrm{TM}}_{\lambda}(\rho,\phi,z) = \frac{1}{2\pi}\left[\frac{i\kappa}{\omega}\frac{J'_m(k\rho)Y_m(kR)-Y'_m(k\rho)J_m(kR)}{\sqrt{J^2_m(kR)+Y^2_m(kR)}}\hat{\mathbf{e}}_\rho - \frac{m\kappa}{\omega k\rho}\frac{J_m(k\rho)Y_m(kR)-Y_m(k\rho)J_m(kR)}{\sqrt{J^2_m(kR)+Y^2_m(kR)}}\hat{\mathbf{e}}_\phi + \frac{k}{\omega}\frac{J_m(k\rho)Y_m(kR)-Y_m(k\rho)J_m(kR)}{\sqrt{J^2_m(kR)+Y^2_m(kR)}}\hat{\mathbf{e}}_z\right]e^{im\phi+i\kappa z}. \tag{16}$$

These mode functions can now be substituted into Eq. (6) for obtaining the energy shift of an atom positioned at $\mathbf{r}=(\rho,\phi,z)$. However, what we want to calculate here is only the correction to the energy shift caused by the presence of a perfectly conducting surface rather than the whole energy shift due to the coupling of the atom to the fluctuating vacuum field, which would include the free-space Lamb shift. Therefore we need to subtract the energy shift caused by the vacuum fluctuations of the electromagnetic field in free space, which is obtained by either letting the phase shifts $\delta_m\to 0$ or equivalently taking the limit $R\to 0$. In the limit of vanishing radius R of the cylinder, the behavior of mode functions (15) and (16) is dominated by the singular behavior of $Y_m(kR)$ and $Y'_m(kR)$ at the origin, which causes the phase shifts [Eq. (14)] to vanish. The renormalized energy shift $\Delta W^{\mathrm{ren}}=\Delta W-\lim_{R\to 0}\Delta W$ is found to be of the form

$$\Delta W^{\mathrm{ren}} = -\frac{1}{4\pi\varepsilon_0}\sum_{j\neq i}(\Xi_\rho|\mu_\rho|^2+\Xi_\phi|\mu_\phi|^2+\Xi_z|\mu_z|^2), \tag{17}$$

with

$$\Xi_\rho = \frac{2}{\pi}{\sum_{m=0}^{\infty}}' \int_0^\infty dkk\int_0^\infty d\kappa\frac{\omega}{E_{ji}+\omega} \times\left\{\left(\frac{m}{k\rho}\right)^2\left\{\frac{[J_m(k\rho)Y'_m(kR)-Y_m(k\rho)J'_m(kR)]^2}{J'^2_m(kR)+Y'^2_m(kR)} - J^2_m(k\rho)\right\} + \left(\frac{\kappa}{\omega}\right)^2 \times\left\{\frac{[J'_m(k\rho)Y_m(kR)-Y'_m(k\rho)J_m(kR)]^2}{J^2_m(kR)+Y^2_m(kR)} - J'^2_m(k\rho)\right\}\right\}, \tag{18}$$

$$\Xi_\phi = \frac{2}{\pi}{\sum_{m=0}^{\infty}}' \int_0^\infty dkk\int_0^\infty d\kappa\frac{\omega}{E_{ji}+\omega} \times\left\{\frac{[J'_m(k\rho)Y'_m(kR)-Y'_m(k\rho)J'_m(kR)]^2}{J'^2_m(kR)+Y'^2_m(kR)} - J'^2_m(k\rho)\right\} + \left(\frac{m}{k\rho}\frac{\kappa}{\omega}\right)^2 \times\left\{\frac{[J_m(k\rho)Y_m(kR)-Y_m(k\rho)J_m(kR)]^2}{J^2_m(kR)+Y^2_m(kR)} - J^2_m(k\rho)\right\}, \tag{19}$$

$$\Xi_z = \frac{2}{\pi}{\sum_{m=0}^{\infty}}' \int_0^\infty dkk\int_0^\infty d\kappa\frac{\omega}{E_{ji}+\omega} \times\left\{\left(\frac{k}{\omega}\right)^2\left\{\frac{[J_m(k\rho)Y_m(kR)-Y_m(k\rho)J_m(kR)]^2}{J^2_m(kR)+Y^2_m(kR)} - J^2_m(k\rho)\right\}\right\}, \tag{20}$$

where the primes on the sums indicate that the $m=0$ term is weighted by an additional factor of 1/2. It appears that the κ integrals fail to converge but this is a common feature in such calculations caused by the dipole approximation, see, e.g., [2]. As we shall see, convergence is in fact brought about by the Bessel functions, which come to bear if the k integral is replaced by an integral over $\omega=\sqrt{\kappa^2+k^2}$.

As the Bessel functions $J_m(x)$ and $Y_m(x)$ are both oscillatory for large x, we wish to rotate the integration contour in

the complex k plane in order to get an integrand that is exponentially damped for large arguments. To this end we introduce the Hankel functions $H_m^{(1)}(x)=J_m(x)+iY_m(x)$ and $H_m^{(2)}(x)=[H_m^{(1)}(x)]^*=J_m(x)-iY_m(x)$, in terms of which we can rewrite the energy-level shift in such a form that there are no poles in the first quadrant of the complex k plane, as is required for the rotation of the integration contour. This step greatly simplifies further analysis,

$$\Xi_\rho = -\mathrm{Re}\frac{2}{\pi}{\sum_{m=0}^{\infty}}' \int_0^\infty dkk \int_0^\infty d\kappa \frac{\omega}{E_{ji}+\omega}\left\{\frac{\kappa^2}{\omega^2}[H_m'^{(1)}(k\rho)]^2 \times \frac{J_m(kR)}{H_m^{(1)}(kR)} + \frac{m^2}{k^2\rho^2}[H_m^{(1)}(k\rho)]^2 \frac{J_m'(kR)}{H_m'^{(1)}(kR)}\right\}, \tag{21}$$

$$\Xi_\phi = -\mathrm{Re}\frac{2}{\pi}{\sum_{m=0}^{\infty}}' \int_0^\infty dkk \int_0^\infty d\kappa \frac{\omega}{E_{ji}+\omega}\left\{[H_m'^{(1)}(k\rho)]^2 \times \frac{J_m'(kR)}{H_m'^{(1)}(kR)} + \frac{m^2}{k^2\rho^2}\frac{\kappa^2}{\omega^2}[H_m^{(1)}(k\rho)]^2 \frac{J_m(kR)}{H_m^{(1)}(kR)}\right\}, \tag{22}$$

$$\Xi_z = -\mathrm{Re}\frac{2}{\pi}{\sum_{m=0}^{\infty}}' \int_0^\infty dkk \int_0^\infty d\kappa \frac{\omega}{E_{ji}+\omega}\left\{\frac{k^2}{\omega^2}[H_m^{(1)}(k\rho)]^2 \times \frac{J_m(kR)}{H_m^{(1)}(kR)}\right\}. \tag{23}$$

We now transform the k integration in Eqs. (21)–(23) into an integration over $\omega=\sqrt{\kappa^2+k^2}$, and note that on the interval $0 \le \omega \le \kappa$ the integrands become pure imaginary and therefore do not contribute if added to the real part of the integral. We can therefore shift the lower limit down to the origin

$$\int_\kappa^\infty d\omega \to \int_0^\infty d\omega, \tag{24}$$

without affecting the result. Further, we note that the functions $H_m^{(1)}(z)$ and $H_m'^{(1)}(z)$ have no zeros in the first quadrant of the complex plane (Fig. 9.6 of [19]) so that the contour of the ω integration can be rotated from the positive real to the positive imaginary axis, $\omega \to i\omega$. Then the oscillatory Bessel functions turn into the modified Bessel functions according to Eqs. 9.6.3 and 9.6.5 of [19]

$$J_m(iz) = e^{im\pi/2} I_m(z), \tag{25}$$

$$H_m^{(1)}(iz) = -\frac{2i}{\pi} e^{-im\pi/2} K_m(z). \tag{26}$$

Taking the real part and going to polar coordinates, where the angle integrals are elementary, we find that

$$\Xi_\rho = \frac{2}{\pi}{\sum_{m=0}^{\infty}}' \int_0^\infty dkk \left\{(\sqrt{E_{ji}^2+k^2}-E_{ji})\frac{I_m(kR)}{K_m(kR)}[K_m'(k\rho)]^2 + \frac{m^2}{k^2\rho^2}\left(\frac{E_{ji}^2}{\sqrt{E_{ji}^2+k^2}}-E_{ji}\right)\frac{I_m'(kR)}{K_m'(kR)}[K_m(k\rho)]^2\right\}, \tag{27}$$

$$\Xi_\phi = \frac{2}{\pi}{\sum_{m=0}^{\infty}}' \int_0^\infty dkk \left\{\left(\frac{E_{ji}^2}{\sqrt{E_{ji}^2+k^2}}-E_{ji}\right)\frac{I_m'(kR)}{K_m'(kR)}[K_m'(k\rho)]^2 + \frac{m^2}{k^2\rho^2}(\sqrt{E_{ji}^2+k^2}-E_{ji})\frac{I_m(kR)}{K_m(kR)}[K_m(k\rho)]^2\right\}, \tag{28}$$

$$\Xi_z = \frac{2}{\pi}{\sum_{m=0}^{\infty}}' \int_0^\infty dkk \left\{\frac{k^2}{\sqrt{E_{ji}^2+k^2}}\frac{I_m(kR)}{K_m(kR)}[K_m(k\rho)]^2\right\}. \tag{29}$$

Note that the effect of our manipulations has been that the integration variable k in Eqs. (27)–(29) has been rotated by $\pi/2$ in the complex plane compared to Eqs. (21)–(23).

The final result for the energy shift, Eq. (17) with Eqs. (27)–(29), is a sum over a series of rapidly converging integrals, which, unlike Eqs. (18)–(20), is reasonably easily evaluated numerically. However, as the functions $\Xi_{\rho,\phi,z}(E_{ji},d,R)$ are quite cumbersome and it is not possible to find exact closed-form expressions for them, we now look at their asymptotics in various limiting cases, which is very useful for analytical estimates.

A. Asymptotic regimes

There are three length scales in the problem: the distance of the atom from the surface of the cylinder $d=\rho-R$, the radius of the cylindrical wire R, and the wavelength of a typical transition in the atom $\lambda_{ji} \propto 1/E_{ji}$. Accordingly we get six different asymptotic regimes, three nonretarded and three retarded. The criterion as to whether retardation matters is the relative size of the distance d of the atom from the surface and the wavelength λ_{ji} of a typical transition: if the atom is very close to the surface its interaction with the surface is entirely electrostatic [1], whereas retardation begins to play a role once $d \sim \lambda_{ji}$ or larger because the internal state of the atom is then subject to non-negligible evolution during the time a virtual photon mediating the interaction would take to travel from the atom to the surface and back. First we shall deal with the three nonretarded cases, and then with the three retarded ones.

1. $d \ll R \ll \lambda_{ji}$

If λ_{ji} is larger than any other length scale, we can take the limit $E_{ji} \to 0$ in Eqs. (27)–(29). This gives the same result as a purely electrostatic calculation [1]. If the distance d of the atom from the surface is small, then the atom does not feel the curvature of the surface, and one expects to get the same energy shift as one would close to a plane surface. This is indeed the result we get when we take the limit $d \to 0$ by using uniform asymptotic expansions for the Bessel functions [1]; we obtain

$$\Xi_\rho \approx \frac{1}{8d^3}, \quad \Xi_\phi \approx \frac{1}{16d^3}, \quad \Xi_z \approx \frac{1}{16d^3}. \tag{30}$$

2. $d \ll \lambda_{ji} \ll R$

In this regime the energy shift behaves in exactly the same way as in the previous case because the radius of the

wire has no influence on retardation so that the relative size of R and λ_{ji} does not matter. All that matters is that the distance d of the atom from the cylinder is still much less than the wavelength λ_{ji} of the relevant transition in the atom. In mathematical terms, the electrostatic limit ($E_{ji}\to 0$) and the large-radius limit ($R\to\infty$) of the energy shift commute.

The limit of large radius was studied in great detail in [6]. Application of the summation formula derived in Appendix A of [6] to Eqs. (27)–(29) leads to the original Casimir-Polder result [2] for the interaction between an atom and a plane, perfectly reflecting mirror:

$$\Xi_\rho = \frac{1}{2\pi d^3}\int_0^\infty d\eta \frac{e^{-2dE_{ji}\eta}}{(1+\eta^2)^2}, \tag{31}$$

$$\Xi_\phi = \Xi_z = \frac{1}{2\pi d^3}\int_0^\infty d\eta \frac{e^{-2dE_{ji}\eta}}{(1+\eta^2)^2}\frac{1-\eta^2}{1+\eta^2}. \tag{32}$$

If we now take λ_{ji} to be much greater than d, we reproduce result (30) of the previous section.

3. $R \ll d \ll \lambda_{ji}$

In this case we again start by taking the limit $E_{ji}\to 0$ in Eqs. (27)–(29) and obtain the electrostatic expression derived in [1]. In the limit of the radius of the wire being much smaller than the distance d, the energy shift is dominated by summand with lowest m in Eqs. (27)–(29) [1]. Asymptotically one gets

$$\Xi_\rho \propto \frac{1}{d^3 \ln d}, \quad \Xi_\phi \propto \frac{R^2}{d^5}, \quad \Xi_z \propto \frac{1}{d^3 \ln d},$$

which is not very helpful numerically as logarithmic series converge only very slowly.

4. $\lambda_{ji} \ll d \ll R$

When λ_{ji} is smaller than the distance d of the atom to the surface of the wire, then the interaction is manifestly retarded. As λ_{ji} is the smallest of the three length scales, we first take the limit $\lambda_{ji}\to 0$, i.e., $E_{ji}\to\infty$, in Eqs. (27)–(29) and find that the leading terms in all three integrals go as $1/E_{ji}$. Thus energy shift (17) indeed depends only the static polarizability (8) of the atom, as mentioned at the end of Sec. II. The remaining integration over k is then quite similar to those found in the nonrelativistic calculation in [1] and can be tackled by the same means. Scaling k to $x=k\rho/m$ and realizing that the dominant contributions to the integrals and sums come from large x and large m, one can approximate the Bessel functions by their uniform asymptotic expansions and then get a geometric series, which is easy to sum. In this way one finds the following approximations

$$\Xi_\rho \approx \frac{1}{2\pi E_{ji}\rho^4}\left\{\rho^4\int_0^\infty dk k^3 \frac{I_0(kR)}{K_0(kR)}[K_1(k\rho)]^2 + \int_0^\infty dx x\left(\sqrt{1+x^2}+\frac{1}{\sqrt{1+x^2}}\right)\frac{A(A^2+4A+1)}{(A-1)^4}\right\}, \tag{33}$$

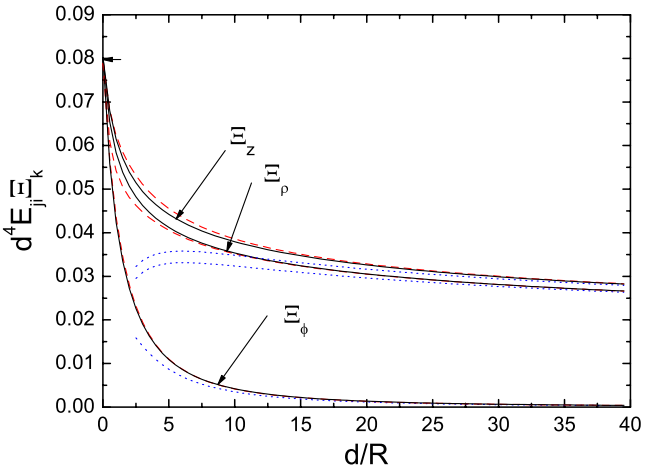

FIG. 2. (Color online) The contributions to the energy shift in the retarded limit due to the three components of the atomic dipole, multiplied by $E_{ji}d^4$. Solid lines represent the results of exact numerical integration of Eqs. (27)–(29) in the limit $E_{ji}\to\infty$, whereas the dashed (red) lines represent approximations (33)–(35). For large d the asymptotic behavior is dominated by the lowest m terms in the sums, given by Eqs. (38)–(40) and shown as dotted (blue) lines. The arrow on the vertical axis indicates the exact value in the limit $d\to 0$, Eq. (37).

$$\Xi_\phi \approx \frac{1}{2\pi E_{ji}\rho^4}\left\{\rho^4\int_0^\infty dk k^3 \frac{I_1(kR)}{K_1(kR)}[K_1(k\rho)]^2 + \int_0^\infty dx x\left(\sqrt{1+x^2}+\frac{1}{\sqrt{1+x^2}}\right)\frac{A(A^2+4A+1)}{(A-1)^4}\right\}, \tag{34}$$

$$\Xi_z \approx \frac{1}{\pi E_{ji}\rho^4}\left\{\rho^4\int_0^\infty dk k^3 \frac{I_0(kR)}{K_0(kR)}[K_0(k\rho)]^2 + \int_0^\infty dx \frac{x^3}{\sqrt{1+x^2}}\frac{A(A^2+4A+1)}{(A-1)^4}\right\}, \tag{35}$$

with $A(x)$ given by

$$A(x) = \left(\frac{R}{\rho}\right)^2\left(\frac{1+\sqrt{1+x^2}}{1+\sqrt{1+x^2\frac{R^2}{\rho^2}}}\right)^2\left[2\left(\sqrt{1+x^2\frac{R^2}{\rho^2}}-\sqrt{1+x^2}\right)\right]. \tag{36}$$

These are easy to evaluate numerically and provide a reasonable approximation to the energy shift in the retarded limit, as shown in Fig. 2. In the limit of the distance $d=\rho-R$ being much smaller than the radius R of the wire, the above approximations yield

$$\Xi_\rho \approx \Xi_\phi \approx \Xi_z \approx \frac{1}{4\pi d^4}\frac{1}{E_{ji}}, \tag{37}$$

which agrees with the retarded energy shift of an atom in front of a perfectly reflecting plane mirror, as calculated by

Casimir and Polder [2]. This is what one would expect because an atom that is very close to the surface is not susceptible to the curvature of the surface.

5. $\lambda_{ji} \ll R \ll d$

In this case we again start by taking the limit $E_{ji} \to \infty$ in Eqs. (27)–(29), which gives a leading-order contribution proportional to $1/E_{ji}$. In other words, this is again a fully retarded case for which the static polarizability (8) is the only atomic property that the energy shift depends on. For distances d much larger than the wire radius R the dominant contribution to the sum then comes from the summands with the lowest m so that we need to consider only those,

$$\Xi_\rho \approx \frac{1}{2\pi E_{ji}} \left\{ \int_0^\infty dk k^3 \frac{I_0(kR)}{K_0(kR)} [K_1(k\rho)]^2 - 2\int_0^\infty dk \frac{k}{\rho^2} \frac{I_1'(kR)}{K_1'(kR)} [K_1(k\rho)]^2 \right\}, \tag{38}$$

$$\Xi_\phi \approx \frac{1}{2\pi E_{ji}} \left\{ \int_0^\infty dk k \left(k^2 + \frac{2}{\rho^2} \right) \frac{I_1(kR)}{K_1(kR)} [K_1(k\rho)]^2 - 2\int_0^\infty dk k^3 \frac{I_1'(kR)}{K_1'(kR)} [K_1'(k\rho)]^2 \right\}, \tag{39}$$

$$\Xi_z \approx \frac{1}{\pi E_{ji}} \int_0^\infty dk k^3 \frac{I_0(kR)}{K_0(kR)} [K_0(k\rho)]^2. \tag{40}$$

The dotted lines in Fig. 2 show that these are indeed good approximations for large d/R. Their leading-order behavior is

$$\Xi_\rho \propto \frac{1}{E_{ji}} \frac{1}{d^4 \ln d}, \quad \Xi_\phi \propto \frac{1}{E_{ji}} \frac{R^2}{d^6}, \quad \Xi_z \propto \frac{1}{E_{ji}} \frac{1}{d^4 \ln d},$$

which is in full agreement with the asymptotic results by [3], even though those are for a metallic wire characterized by a plasma frequency. This is because in the retarded limit the interaction between the atom and the surface depends, to leading order, only on the static polarizability.

As in the electrostatic case, the contributions due to the ρ and z components of the atomic dipole fall off less rapidly than the ϕ contribution. We also note that, just as in the nonretarded case, the series in powers of $1/\ln d$ converge too slowly to be of any practical use so that estimates must be made with Eqs. (38)–(40).

6. $R \ll \lambda_{ji} \ll d$

As in the nonretarded cases, the limit of vanishing radius ($R \to 0$) and the retarded limit ($E_{ji} \to \infty$) commute, and we recover the results of the previous section, Eqs. (38)–(40). This is another manifestation of the fact that the criterion of whether the interaction is retarded depends solely on the distance d between an atom and the surface of the wire, and that the relative size of geometrical features and the wavelength λ_{ji} is irrelevant. This means in particular that there are no resonance effects for λ_{ji} coinciding with the wire radius R.

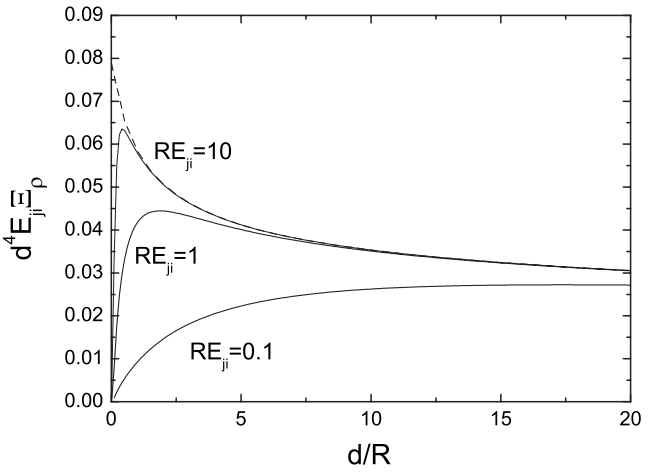

FIG. 3. Contribution (27) to energy shift (17) due to the ρ component of the dipole for various typical transition frequencies E_{ji}. The dashed line is this contribution in the retarded limit $E_{ji} \to \infty$.

B. Numerical results

For intermediate parameter ranges one has to evaluate Eqs. (27)–(29) numerically. This is straightforward, and one can employ standard software packages such as MATHEMATICA or MAPLE. The numerical convergence of Eqs. (27)–(29) is very good although more terms are needed for small distances d than for large distances. Figures 3–5 show the contributions by the ρ, ϕ, and z components of the atomic dipole to energy shift (17) for various values of the typical transition frequency E_{ji} in the atom. We give the distance d and the transition wavelength $1/E_{ji}$ in units of the wire radius R. For plotting we have factored out of $\Xi_{\rho,\phi,z}$ the asymptotic functional dependence of the shift in front of a plane mirror, Eq. (37).

In Fig. 6 we show how these contributions look when we choose the wavelengths $1/E_{ji}$ of a typical internal transition as a length scale and plot the contributions to the energy shift

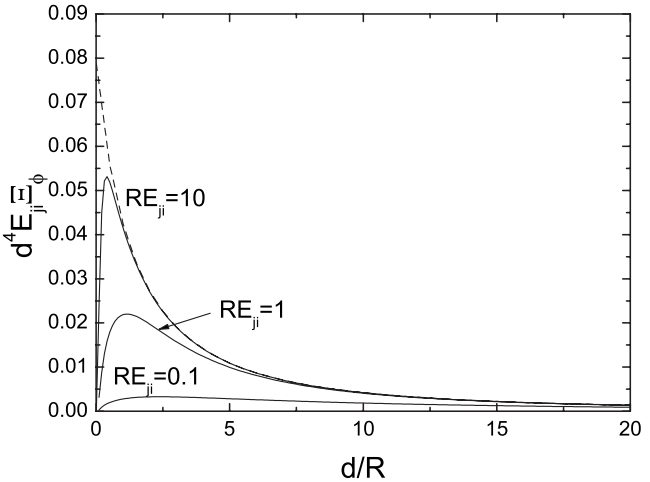

FIG. 4. Contribution (28) to energy shift (17) due to the ϕ component of the dipole for various typical transition frequencies E_{ji}. The dashed line is this contribution in the retarded limit $E_{ji} \to \infty$.

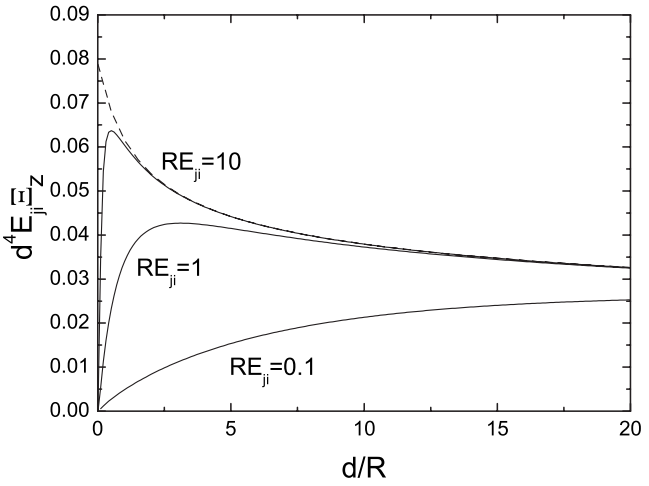

FIG. 5. Contribution (29) to energy shift (17) due to the z component of the dipole for various typical transition frequencies E_{ji}. The dashed line is this contribution in the retarded limit $E_{ji}\to\infty$.

for various wire radii R. The larger the value of R the more terms are required in the numerical series.

IV. ENERGY SHIFT NEAR A PERFECTLY REFLECTING SEMI-INFINITE HALF-PLANE

Next we wish to calculate the energy shift of an atom in the vicinity of a perfectly reflecting half-plane, as illustrated by Fig. 7.

The procedure of obtaining the normal modes of the vector potential is analogous to that described in Sec. III. The scalar solution of the Helmholtz equation (4) in cylindrical coordinates that is best suited to applying boundary conditions on the surface of the half-plane is given by

$$\Phi(\mathbf{x}) = \left[\frac{\alpha}{\sqrt{\pi}}\sin\left(\frac{m}{2}\phi\right) + \frac{\beta}{\sqrt{\pi}}\cos\left(\frac{m}{2}\phi\right)\right] J_{m/2}(k\rho)\frac{e^{i\kappa z}}{\sqrt{2\pi}},$$

where $J_{m/2}(k\rho)$, with $m=0,1,2,\ldots$, are the regular solutions of Bessel's equation, and the separation constants satisfy

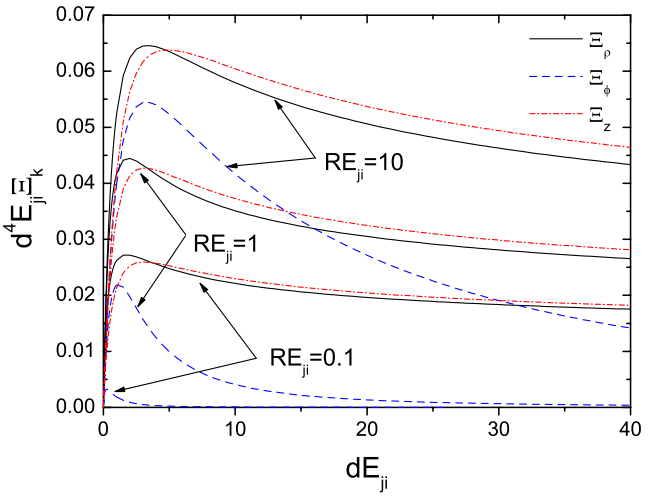

FIG. 6. (Color online) Contributions (27)–(29) to energy shift (17) due to the ρ, ϕ, and z components of the dipole for various radii R of the wire.

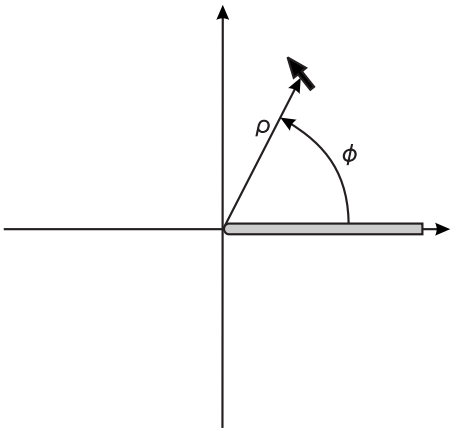

FIG. 7. An atomic dipole in the vicinity of a perfectly reflecting semi-infinite half-plane. The normal modes $\mathbf{F}_\lambda^{(\sigma)}(\mathbf{x})$ in this geometry are given by Eqs. (41) and (42).

$\omega^2=k^2+\kappa^2$. We must have $m\geq 0$, as otherwise the solutions are not linearly independent. Note that half-integer indices arise because the angle ϕ is restricted to the interval $[0,2\pi]$ so that the usual argument of single-valuedness of $e^{im\phi}$ cannot be evoked.

In order to obtain two linearly independent vector solutions, we again apply Eqs. (10) and (11), and impose the boundary conditions for a perfectly reflecting half-plane, $E_\rho=0=E_z$ and $B_\phi=0$ for $\phi=0$ and $\phi=2\pi$. In this way we find for the mode functions

$$\mathbf{F}_\lambda^{(1)}(\mathbf{r}) = -\frac{1}{\sqrt{2\pi}}\left[\frac{m}{2k\rho}\sin\left(\frac{m}{2}\phi\right)J_{m/2}(k\rho)\hat{\mathbf{e}}_\rho + \cos\left(\frac{m}{2}\phi\right)J'_{m/2}(k\rho)\hat{\mathbf{e}}_\phi\right]e^{i\kappa z}, \tag{41}$$

$$\mathbf{F}_\lambda^{(2)}(\mathbf{r}) = \frac{1}{\sqrt{2\pi}}\left[\frac{i\kappa}{\omega}\sin\left(\frac{m}{2}\phi\right)J'_{m/2}(k\rho)\hat{\mathbf{e}}_\rho + \frac{i\kappa m}{2k\rho\omega}\cos\left(\frac{m}{2}\phi\right)J_{m/2}(k\rho)\hat{\mathbf{e}}_\phi + \frac{k}{\omega}\sin\left(\frac{m}{2}\phi\right)J_{m/2}(k\rho)\hat{\mathbf{e}}_z\right]e^{i\kappa z}, \tag{42}$$

where the composite index stands for $\lambda=\{k,m,\kappa\}$. For $m>0$ these mode functions satisfy normalization condition (13) but the first polarization has an additional mode with $m=0$ for which Eq. (41) must be multiplied by an additional factor of $1/\sqrt{2}$ for it to be normalized correctly according to Eq. (13),

$$\mathbf{F}_{m=0}^{(1)}(\mathbf{r}) = -\frac{1}{2\pi}J'_0(k\rho)\hat{\mathbf{e}}_\phi e^{i\kappa z}. \tag{43}$$

Substituting mode functions (41)–(43) into Eq. (6) and renormalizing the energy shift by subtracting the free-space contribution in the same way as this was done in Eqs. (18)–(20), we obtain an energy shift of form (17) with

$$\Xi_\rho = \frac{2}{\pi}\int_0^\infty dkk \int_0^\infty d\kappa \frac{\omega}{E_{ji}+\omega} \times \left\{ \left(\frac{1}{k\rho}\right)^2 \sum_{m=1}^{\infty} \left[\left(\frac{m}{2}\right)^2 \sin^2\left(\frac{m}{2}\phi\right) J_{m/2}^2(k\rho) - m^2 J_m^2(k\rho) \right] + \left(\frac{\kappa}{\omega}\right)^2 \sum_{m=0}^{\infty}{}' \left[\sin^2\left(\frac{m}{2}\phi\right) J_{m/2}'^2(k\rho) - J_m'^2(k\rho) \right] \right\}, \quad (44)$$

$$\Xi_\phi = \frac{2}{\pi}\int_0^\infty dkk \int_0^\infty d\kappa \frac{\omega}{E_{ji}+\omega} \left\{ \sum_{m=0}^{\infty}{}' \left[\cos^2\left(\frac{m}{2}\phi\right) J_{m/2}'^2(k\rho) - J_m'^2(k\rho) \right] + \left(\frac{\kappa}{k\rho\omega}\right)^2 \sum_{m=1}^{\infty} \left[\left(\frac{m}{2}\right)^2 \cos^2\left(\frac{m}{2}\phi\right) J_{m/2}^2(k\rho) - m^2 J_m^2(k\rho) \right] \right\}, \quad (45)$$

$$\Xi_z = \frac{2}{\pi}\int_0^\infty dkk \int_0^\infty d\kappa \frac{\omega}{E_{ji}+\omega} \left\{ \left(\frac{k}{\omega}\right)^2 \sum_{m=0}^{\infty}{}' \left[\sin^2\left(\frac{m}{2}\phi\right) \times J_{m/2}^2(k\rho) - J_m^2(k\rho) \right] \right\}, \quad (46)$$

where the primes on the sums indicate that the $m=0$ terms are weighted by an additional factor of 1/2. In order to simplify these expressions, the sums over the Bessel functions need to be evaluated. Recently, similar summations have been carried out [16,20] but the results obtained do not include our particular case of sums involving Bessel functions of the half-integer order.

We proceed along the following lines. First, we split each sum into two, one over Bessel functions of integer orders, and the other over half-integer orders. For the first we can apply the standard summation formula {Eq. 9.1.79 of [19]}

$$\sum_{m=0}^{\infty}{}' \cos(2m\phi) J_m^2(z) = \frac{1}{2} J_0(2z\sin\phi), \quad (47)$$

and we choose to represent the right-hand side in terms of an integral {Eq. 9.1.24 of [19]}

$$\frac{1}{2} J_0(2z\sin\phi) = \frac{1}{\pi}\int_1^\infty dt \frac{\sin(2zt\sin\phi)}{\sqrt{t^2-1}}. \quad (48)$$

For the half-integer sum we use a summation formula of Eq. 5.7.17.(11.) from [21], which in our case gives

$$\sum_{m=0}^{\infty} \cos(2m+1)\phi J_{m+(1/2)}^2(z) = \frac{1}{\pi}\int_1^{1/\sin\phi} dt \frac{\sin(2zt\sin\phi)}{\sqrt{t^2-1}}. \quad (49)$$

We note that, if we use integral representation (48), the sums over integer and over half-integer Bessel functions are very similar; the only difference is the upper limit of the t integral in Eqs. (48) and (49). As these t integrals and their derivatives will arise repeatedly, we define the following auxiliary functions:

$$F(z,\phi) \equiv \int_1^{1/\sin\phi} dt \frac{\sin(2zt\sin\phi)}{\sqrt{t^2-1}}, \quad (50)$$

$$G(z,\phi) \equiv \int_1^{\infty} dt \frac{\sin(2zt\sin\phi)}{\sqrt{t^2-1}}. \quad (51)$$

Further, we note that the κ integrals in Eqs. (44)–(46) suffer from the same convergence problems as already discussed in Sec. III. We avoid these by introducing polar coordinates with $k=\omega\sin\alpha$ and $\kappa=\omega\cos\alpha$. At the same time we parametrize the denominator arising from perturbation theory by

$$\frac{1}{E_{ji}+\omega} = \int_0^\infty dx e^{-(E_{ji}+\omega)x}, \quad (52)$$

with $E_{ji}+\omega = E_{ji}+\sqrt{k^2+\kappa^2} \geq 0$. Then Eqs. (44)–(46) become

$$\Xi_\rho = \frac{2}{\pi}\int_0^\infty dx e^{-E_{ji}x} \int_0^\infty d\omega\omega^3 e^{-\omega x} \int_0^{\pi/2} d\alpha \sin\alpha \{\sigma_1(\omega\rho\sin\alpha) + \sigma_3(\omega\rho\sin\alpha)\cos^2\alpha\}, \quad (53)$$

$$\Xi_\phi = \frac{2}{\pi}\int_0^\infty dx e^{-E_{ji}x} \int_0^\infty d\omega\omega^3 e^{-\omega x} \int_0^{\pi/2} d\alpha \times \sin\alpha \{\sigma_2(\omega\rho\sin\alpha)\cos^2\alpha + \sigma_4(\omega\rho\sin\alpha)\}, \quad (54)$$

$$\Xi_z = \frac{2}{\pi}\int_0^\infty dx e^{-E_{ji}x} \int_0^\infty d\omega\omega^3 e^{-\omega x} \int_0^{\pi/2} d\alpha \times \sin\alpha \{\sigma_5(\omega\rho\sin\alpha)\sin^2\alpha\}. \quad (55)$$

The sums $\sigma_i(z)$ appearing in these expressions can be calculated by using Eqs. (47)–(51) and standard derivative formulas for Bessel functions {Eq. 9.1.27 of [19]}; we obtain in terms of Eqs. (50) and (51):

$$\left.\begin{matrix}\sigma_1(z)\\ \sigma_2(z)\end{matrix}\right\} = \frac{1}{z^2}\sum_{m=1}^{\infty} \times \left[\left(\frac{m}{2}\right)^2 \left\{ \begin{matrix}\sin^2(m\phi/2)\\ \cos^2(m\phi/2)\end{matrix} \right\} J_{m/2}^2(z) - m^2 J_m^2(z) \right] = \frac{1}{8\pi z^2}\left[\pm \frac{\partial^2 G(z,\phi)}{\partial\phi^2} + \left.\frac{\partial^2 G(z,\phi)}{\partial\phi^2}\right|_{\phi=0} \pm \frac{\partial^2 F(z,\phi)}{\partial\phi^2} - \left.\frac{\partial^2 F(z,\phi)}{\partial\phi^2}\right|_{\phi=0} \right], \quad (56)$$

$$\left.\begin{matrix}\sigma_3(z)\\ \sigma_4(z)\end{matrix}\right\} = \sum_{m=0}^{\infty}{}' \left[\left\{\begin{matrix}\sin^2(m\phi/2)\\ \cos^2(m\phi/2)\end{matrix}\right\} J'^2_{m/2}(z) - J'^2_m(z)\right]$$
$$= -\left\{\begin{matrix}\sigma_1(z)\\ \sigma_2(z)\end{matrix}\right\} + \frac{1}{2\pi}[F(z,0) - G(z,0)] \mp \frac{\cos 2\phi}{2\pi}[F(z,\phi) + G(z,\phi)] + \frac{\cos 2z}{2\pi z}(1 \mp \cos\phi), \quad (57)$$

$$\sigma_5(z) = \sum_{m=0}^{\infty}{}' \{\sin^2(m\phi/2) J^2_{m/2}(z) - J^2_m(z)\}$$
$$= \frac{1}{2\pi}[F(z,0) - F(z,\phi) - G(z,\phi) - G(z,0)]. \quad (58)$$

We now carry out the various integrations in the following order. First we evaluate the α integrals, which all give Bessel functions J_1 or J_0 {cf. Eqs. 3.715(10),(14) [18]}. Next we carry out the integrations over ω, which involve integrals of the type {Eq. 6.611(1) of [18]}

$$\int_0^\infty dz e^{-az} J_\nu(bz) = \frac{b^{-\nu}(\sqrt{a^2+b^2}-a)^\nu}{\sqrt{a^2+b^2}}.$$

Finally, we calculate the t integrals that came in through the auxiliary functions F and G [Eqs. (50) and (51)]. These are all elementary. At the very end we calculate the ϕ derivatives of Eq. (56) and take the limit $\phi \to 0$ in the appropriate terms. The end results then still contain the parameter integral (52) over x, which we now scale by substituting $x = 2\rho\eta$. Then the final results read

$$\Xi_\rho = \frac{1}{16\pi\rho^3}\int_0^\infty d\eta e^{-2\rho E_{ji}\eta}\left\{\frac{3\eta^4+6\eta^2+4}{\eta^4(1+\eta^2)^{3/2}} - \frac{4}{\eta^4} + \frac{4}{(\eta^2+\sin^2\phi)^3}[(2\eta^2+1)\sin^2\phi - \eta^2] + \frac{\cos\phi}{(1+\eta^2)^{3/2}(\eta^2+\sin^2\phi)^3}[(2+\eta^2)\sin^4\phi + 2\sin^2\phi(3\eta^4+6\eta^2+2) - \eta^2(3\eta^4+6\eta^2+4)]\right\}, \quad (59)$$

$$\Xi_\phi = \frac{1}{16\pi\rho^3}\int_0^\infty d\eta e^{-2\rho E_{ji}\eta}\left\{\frac{3\eta^6+6\eta^4+10\eta^2+4}{\eta^4(1+\eta^2)^{5/2}} - \frac{4}{\eta^4} + \frac{4}{(\eta^2+\sin^2\phi)^3}[(1-2\eta^2)\sin^2\phi + \eta^2] + \frac{\cos\phi}{(1+\eta^2)^{5/2}(\eta^2+\sin^2\phi)^3}[(2-2\eta^2-\eta^4)\sin^4\phi + 2\sin^2\phi(2+2\eta^2-6\eta^4-3\eta^6) + \eta^2(3\eta^6 + 6\eta^4+10\eta^2+4)]\right\}, \quad (60)$$

$$\Xi_z = \frac{1}{16\pi\rho^3}\int_0^\infty d\eta e^{-2\rho E_{ji}\eta}\left\{\frac{9\eta^4+10\eta^2+4}{\eta^4(1+\eta^2)^{5/2}} - \frac{4}{\eta^4} + 4\frac{\sin^2\phi-\eta^2}{(\eta^2+\sin^2\phi)^3} - \frac{\cos\phi}{(1+\eta^2)^{5/2}(\eta^2+\sin^2\phi)^3} \times[(\eta^2-2)\sin^4\phi + 2(\eta^4-4\eta^2-2)\sin^2\phi + \eta^2 \times(9\eta^4+10\eta^2+4)]\right\}. \quad (61)$$

Inserted into Eq. (17), Eqs. (59)–(61) give the final result for the energy shift of an atom near a perfectly reflecting half-plane. Some of the integrations over the auxiliary variable η could in principle be carried out but those would yield complicated hypergeometric functions. Thus it is preferable to have the result in the form of an integral over elementary functions. It converges quickly and can therefore be very easily evaluated numerically by using standard software packages. In addition, we shall go on to determine asymptotic expressions in the nonretarded and retarded regimes.

A. Asymptotic regimes

1. Plane-mirror limit

In the limit of the polar angle ϕ being very small, the atom is very close to the half-plane but far away from the edge so that the energy shift should be the same as for an atom in front of a plane, infinitely extended mirror. The component of the atomic dipole that is normal to the surface should then give the contribution listed in Eq. (31) to the shift, and the parallel components should contribute the one that is shown in Eq. (32). As the distance d of the atom from the half-plane is $\rho\sin\phi$, we take Eqs. (59)–(61) and scale $\eta \to \eta\sin\phi$ so as to get an exponential with the same argument as in Eqs. (31) and (32). If we subsequently take the limit $\phi \to 0$, we recover Eqs. (31) and (32), as expected. Note that, however, the geometry is different from the cylindrical case: the ϕ component of the atomic dipole is now normal to the surface and its contribution Ξ_ϕ to the energy shift is given by Eq. (31), and the ρ and z components are parallel so that Ξ_ρ and Ξ_z are given by Eq. (32).

2. Nonretarded regime

If $\rho E_{ji} \ll 1$ then the atom is very close to the half-plane, compared to the wavelength of a typical internal transition. This means that the interaction of the atom and the surface is instantaneous, as the atom evolves on a much longer time scale. In this case field quantization is not necessary, and only Coulomb interactions between the atom and the half-plane need to be considered, as was done in Ref. [1], where we derived

$$\Xi_\rho = \frac{5}{48\pi\rho^3} + \frac{\cos\phi}{16\pi\rho^3\sin^2\phi} + \frac{(\pi-\phi)(1+\sin^2\phi)}{16\pi\rho^3\sin^3\phi},$$

$$\Xi_\phi = -\frac{1}{48\pi\rho^3} + \frac{\cos\phi}{8\pi\rho^3\sin^2\phi} + \frac{(\pi-\phi)(1+\cos^2\phi)}{16\pi\rho^3\sin^3\phi},$$

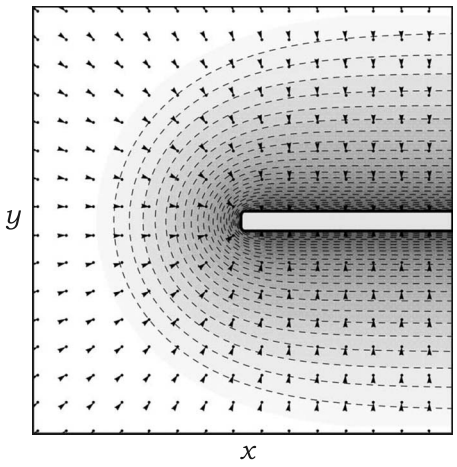

FIG. 8. Direction of the retarded Casimir-Polder force acting on the atom with isotropic polarizability. Note from Eq. (60) that an atom that is polarized azimuthally does not experience any force when it is located exactly above the edge of the half-plane.

$$\Xi_z = \frac{1}{24\pi\rho^3} + \frac{\cos\phi}{16\pi\rho^3\sin^2\phi} + \frac{\pi-\phi}{16\pi\rho^3\sin^3\phi}.$$

Taking the limit $E_{ji}\to 0$ in Eqs. (59)–(61) we recover these results, which is an important consistency check on our present calculation.

3. Retarded regime

In the opposite limit of the atom being far away from the half-plane, we need to distinguish whether the atom is located beyond the edge of the half-plane or not. If it is, i.e., for $\pi/2<\phi<\pi$ the distance of the atom to the half-plane is its distance to the edge, namely, ρ, so that the condition for the interaction to be fully retarded is $\rho E_{ji}\gg 1$. If, on the other hand, $0<\phi<\pi/2$ then the distance to the half-plane is $\rho\sin\phi$, and consequently the criterion for full retardation is $\rho\sin\phi E_{ji}\gg 1$, cf. Fig. 7.

Taking the limit $E_{ji}\to\infty$ in integrals (59)–(61) is straightforward since, according to Watson's lemma [22], the integral is then dominated by contributions from the vicinity of $\eta=0^+$ so that one just needs to factor out the exponential and expand the rest of the integrand in the curly brackets in a Taylor series about this point. The leading terms of these Taylor expansions turn out to be constants with respect to η in each case. Thus in the retarded limit we obtain

$$\Xi_\rho = \frac{1}{64\pi\rho^4 E_{ji}}\left[3+\frac{1}{\sin^4(\phi/2)}+\frac{2}{\sin^2(\phi/2)}\right], \quad (62)$$

$$\Xi_\phi = \frac{1}{64\pi\rho^4 E_{ji}}\left[-3+\frac{1}{\sin^4(\phi/2)}+\frac{2}{\sin^2(\phi/2)}\right], \quad (63)$$

$$\Xi_z = \frac{1}{64\pi\rho^4 E_{ji}}\left[3+\frac{1}{\sin^4(\phi/2)}+\frac{2}{\sin^2(\phi/2)}\right], \quad (64)$$

which, for the case of isotropic polarizability, is in agreement with the result of Ref. [15]. Here again, the energy shift (17) depends only on the static polarizability (8) of the atom, as follows from general considerations in the retarded limit [17]. In the light of our comments above, we emphasize again that results (62)–(64) are only valid when the distance of the atom from the half-plane exceeds several wavelengths λ_{ji}. This means that for small angles ϕ one needs to revert to the plane-mirror limit discussed in Sec. IV A 1 above because, in the region $0<\phi<\pi/2$, Eqs. (62)–(64) apply only if $\sin\phi\gg\lambda_{ji}/\rho$. However, taking the limit $\rho\to\infty$ together with $\phi\to 0$ while keeping $\rho\sin\phi=d$ fixed is legitimate, and reproduces the well-known Casimir-Polder result [2] for the retarded interaction between an atom and a plane mirror, Eq. (37).

Taking the limit $\phi\to\pi$ in Eqs. (62)–(64) shows that for an atomic dipole that is polarized azimuthally the interaction vanishes when the atom is located exactly above the edge of the half-plane (see also Fig. 8). This conclusion actually holds not just in the retarded regime but generally for any distance, as Eq. (60) also vanishes in the limit $\phi\to\pi$. Purely from symmetry one would expect there to be no azimuthal component to the Casimir-Polder force directly above the edge but the fact that there is no radially directed force either is surprising.

Since we have worked in the cylindrical coordinates, the direction of the unit vectors $\hat{\mathbf{e}}_\rho$ and $\hat{\mathbf{e}}_\phi$ depends on the position coordinates ρ and ϕ. In this context it is curious that, in the retarded limit, all three components of the atomic dipole contribute to the energy shift with exactly the same angular dependence.

V. SUMMARY

We have calculated the energy shift in a neutral atom caused by the presence at arbitrary distance of perfectly reflecting microstructures of two different geometries. For an atom at a distance $d=\rho-R$ from the perfectly reflecting cylindrical wire of radius R, we have found an exact expression for the interaction energy, Eq. (17) with Eqs. (27)–(29). As these integrals and sums are in general quite complicated, we have analyzed various important limiting cases. The limit of the distance d being small on the scale of the wavelength λ_{ji} of a typical atomic transition requires only electrostatic forces to be considered, which was done in detail in Ref. [1]. The case of purely retarded interactions, which occur when the distance d is much larger than λ_{ji}, has been analyzed in Secs. III A 4–III A 6. For a small wire radius the three contributions to the energy shift are well approximated by Eqs. (38)–(40), and for a large wire radius by Eqs. (33)–(35).

In the case of an atom close to a perfectly reflecting half-plane, the exact analytic analysis can be pushed a little bit further than in the cylindrical case. We have managed to find an exact formula for the energy shift in terms of a simple rapidly converging integral over elementary functions [Eqs. (59)–(61)] so that they are very easy to study numerically. Nevertheless, we have also derived asymptotic formulas, which agree with previous calculations.

The totality of our results can be used to reliably estimate the energy shift in an atom close to a variety of common microstructures that consist of a ledge and possibly an electroplated top layer of higher reflectivity. We have determined

the energy shifts for the complete range of distances, which is very important for practical applications; as in many modern experiments the distance of the atom is neither much larger nor much smaller than the typical wavelength of an atomic transition but commensurate.

ACKNOWLEDGMENTS

It is a pleasure to thank Gabriel Barton for discussions. We would like to acknowledge financial support from the U.K. Engineering and Physical Sciences Research Council.

[1] C. Eberlein and R. Zietal, Phys. Rev. A **75**, 032516 (2007).
[2] H. B. G. Casimir and D. Polder, Phys. Rev. **73**, 360 (1948).
[3] Yu. S. Barash and A. A. Kyasov, Sov. Phys. JETP **68**, 39 (1989).
[4] Ya. B. Zel'dovich, Zh. Eksp. Teor. Fiz. **5**, 22 (1935).
[5] V. M. Nabutovskii, V. R. Belosludov, and A. M. Korotkikh, Sov. Phys. JETP **50**, 352 (1979).
[6] A. M. Marvin and F. Toigo, Phys. Rev. A **25**, 782 (1982).
[7] M. J. Mehl and W. L. Schaich, Phys. Rev. A **16**, 921 (1977).
[8] M. J. Mehl and W. L. Schaich, Phys. Rev. A **21**, 1177 (1980).
[9] D. Langbein, *Theory of Van der Waals Attraction* (Springer, Berlin, 1974).
[10] A. M. Marvin and F. Toigo, Phys. Rev. A **25**, 803 (1982).
[11] D. P. Fussell, R. C. McPhedran, and C. Martijn de Sterke, Phys. Rev. A **71**, 013815 (2005).
[12] M. Boustimi, J. Baudon, P. Candori, and J. Robert, Phys. Rev. B **65**, 155402 (2002).
[13] M. Boustimi, J. Baudon, and J. Robert, Phys. Rev. B **67**, 045407 (2003).
[14] E. V. Blagov, G. L. Klimchitskaya, and V. M. Mostepanenko, Phys. Rev. B **71**, 235401 (2005).
[15] I. Brevik, M. Lygren, and V. N. Marachewsky, Ann. Phys. (N.Y.) **267**, 134 (1998).
[16] T. N. C. Mendes, F. S. S. da Rosa, A. Tenorio, and C. Farina, J. Phys. A **41**, 164029 (2008).
[17] A. D. McLachlan, Proc. R. Soc. London, Ser. A **271**, 387 (1963).
[18] I. S. Gradshteyn and I. M. Ryzhik, in *Table of Integrals, Series, and Products*, 5th ed., edited by A. Jeffrey (Academic Press, London, 1994).
[19] *Handbook of Mathematical Functions*, edited by M. Abramowitz and I. Stegun (US GPO, Washington, DC, 1964).
[20] F. S. S. Rosa, T. N. C. Mendes, A. Tenorio, and C. Farina, Phys. Rev. A **78**, 012105 (2008).
[21] A. P. Prudnikov, Yu. A. Brychkov, and O. I. Marichev, *Integrals and Series*, 3rd ed. (Gordon and Breach, New York, 1992), Vol. 2.
[22] C. M. Bender and S. A. Orszag, *Advanced Mathematical Methods for Scientists and Engineers* (Springer, Berlin, 1999).